Pflugers Arch - Eur J Physiol (2011) 462:455–467
DOI 10.1007/s00424-011-0981-y

SIGNALING AND CELL PHYSIOLOGY

Epithelial-to-mesenchymal transition in podocytes mediated by activation of NADPH oxidase in hyperhomocysteinemia

Chun Zhang · Min Xia · Krishna M. Boini · Cai-Xia Li · Justine M. Abais · Xiao-Xue Li · Laura A. Laperle · Pin-Lan Li

Received: 15 January 2011 / Revised: 20 April 2011 / Accepted: 23 May 2011 / Published online: 7 June 2011

Abstract The present study tested the hypothesis that hyperhomocysteinemia (hHcys) induces podocytes to undergo epithelial-to-mesenchymal transition (EMT) through the activation of NADPH oxidase (Nox). It was found that increased homocysteine (Hcys) level suppressed the expression of slit diaphragm-associated proteins, P-cadherin and zonula occludens-1 (ZO-1), in conditionally immortalized mouse podocytes, indicating the loss of their epithelial features. Meanwhile, Hcys remarkably increased the abundance of mesenchymal markers, such as fibroblast specific protein-1 (FSP-1) and α-smooth muscle actin (α-SMA). These phenotype changes in podocytes induced by Hcys were accompanied by enhanced superoxide ($O_2^{\cdot-}$) production, which was substantially suppressed by inhibition of Nox activity. Functionally, Hcys significantly enhanced the permeability of the podocyte monolayer coupled with increased EMT, and this EMT-related increase in cell permeability could be restored by Nox inhibitors. In mice lacking $gp91^{phox}$ ($gp91^{-/-}$), an essential Nox subunit gene, hHcys-enhanced podocyte EMT and consequent glomerular injury were examined. In wild-type ($gp91^{+/+}$) mice, hHcys induced by a folate-free diet markedly enhanced expression of mesenchymal markers (FSP-1 and α-SMA) but decreased expression of epithelial markers of podocytes in glomeruli, which were not observed in $gp91^{-/-}$ mouse glomeruli. Podocyte injury, glomerular sclerotic pathology, and marked albuminuria observed in $gp91^{+/+}$ mice with hHcys were all significantly attenuated in $gp91^{-/-}$ mice. These results suggest that hHcys induces EMT of podocytes through activation of Nox, which represents a novel mechanism of hHcys-associated podocyte injury.

Keywords Homocysteinemia · NADPH oxidase · Podocytes · Epithelial-to-mesenchymal transition · End-stage renal disease · Kidney · Albumin · Cellular response · Renal · Differentiation

Introduction

There is considerable evidence showing that hyperhomocysteinemia (hHcys) is importantly implicated in the progression of end-stage renal disease (ESRD) and in the development of cardiovascular complications related to ESRD [8, 24, 31]. Studies from our laboratory [45, 47] and by others [14] have demonstrated that Hcys induces extracellular matrix (ECM) accumulation and inhibits their degradation in mesangial cells, which ultimately leads to glomerulosclerosis and loss of renal function. Although the precise mechanism of hHcys-induced glomerulosclerosis has not yet been fully elucidated, we and others have demonstrated that oxidative stress mediated by NADPH oxidase (Nox) is importantly involved in the progression of glomerular injury associated with hHcys [40, 45]. In addition, recent studies have shown that Nox activation is essential in hHcys-induced podocyte injury, which is a

Electronic supplementary material The online version of this article (doi:10.1007/s00424-011-0981-y) contains supplementary material, which is available to authorized users.

C. Zhang · M. Xia · K. M. Boini · C.-X. Li · J. M. Abais · X.-X. Li · L. A. Laperle · P.-L. Li (✉)
Department of Pharmacology & Toxicology,
Medical College of Virginia, Virginia Commonwealth University,
410 N 12th Street,
Richmond, VA 23298, USA
e-mail: pli@vcu.edu

C. Zhang
Department of Nephrology, Union Hospital, Tongji Medical College,
Huazhong University of Science and Technology,
1277 Jie Fang Avenue,
Wuhan 430022, China

crucial early event that leads to glomerulosclerosis [42]. However, the molecular mechanism mediating hHcys-induced podocyte injury, in particular, how Nox activation causes podocyte dysfunction and initiates glomerulosclerosis, remains poorly understood.

Podocytes are unique glomerular epithelial cells that comprise the outermost layer of the glomerular filtration barrier [16, 17, 28]. Podocyte foot processes interdigitate with the counterparts of neighboring cells to form the slit diaphragm, which constitutes the final barrier to prevent protein loss from vascular to urinary space. It has been reported that any injury to podocytes that disrupts the structural and functional integrity of the slit diaphragm would eventually lead to a defective glomerular filtration, thereby causing proteinuria. Podocyte injury has been considered as the most important early event initiating glomerulosclerosis in different animal models and humans, such as focal segmental glomerulosclerosis, membranous nephropathy, diabetic nephropathy, and lupus nephritis [23, 26, 53]. Therefore, the molecular mechanism producing podocyte injury becomes one of the most important mechanisms in the progression of ESRD due to a variety of causes. In hHcys, podocyte effacement, cytoskeleton reorganization, decreased expression of slit diaphragm molecules, and podocyte apoptosis were documented [49, 50], indicating the occurrence of podocyte injury during hHcys. However, the mechanism by which hHcys induces podocyte injury has not been fully elucidated.

Recently, two major hypotheses have been proposed for podocyte injury under different conditions. The prevalent view emphasizes the importance of podocyte depletion resulting from apoptosis as a causative factor for the onset of proteinuria and glomerulosclerosis [37, 41, 48]. In this hypothesis, the reduced podocyte number in glomeruli is attributed to the apoptotic death of these cells. However, recent studies have shown that the detached podocytes might be alive and could be presented in the urine of some patients with chronic kidney diseases [2, 25, 35]. Therefore, another hypothesis for podocyte injury proposes that injured podocytes could obtain a motile ability facilitating their detachment from the glomerular basement membrane rather than apoptotic cell death. In this context, emerging evidence suggests that podocytes could undergo an epithelial-to-mesenchymal transition (EMT) process when challenged by different injurious stimuli, such as transforming growth factor-β1 (TGF-β1), high glucose, and adriamycin [15]. Although there are still some debates concerning the EMT [18], it has been proposed that the EMT process is characterized by losing its epithelial features, such as nephrin, P-cadherin, and zonula occludens-1 (ZO-1), as well as acquiring mesenchymal features, such as increases in the expression of desmin, fibroblast-specific protein-1 (FSP-1), and α-smooth muscle actin (α-SMA) [3, 20, 21, 32]. This phenotype transition process will render podocytes motile and ultimately lead to disruption of the delicate architecture of these cells, thereby impairing their filtration barrier function and initiating glomerulosclerosis [15]. However, whether hHcys could also induce podocyte EMT and thereby cause glomerulosclerosis is unknown, and the present study attempted to answer this important question.

Given the important role of Nox activation in Hcys-induced glomerular injury, the present study hypothesized that hHcys may induce podocyte EMT through the activation of Nox and subsequent $O_2^{\cdot-}$ production, ultimately leading to hHcys-associated podocyte dysfunction and subsequent glomerulosclerosis. To test this hypothesis, we first used cultured murine podocytes to examine whether they could undergo EMT upon stimulation of Hcys. Then, the effects of Nox inhibition on Hcys-induced phenotypic changes, and their functional relevance were examined. Using mice lacking $gp91^{phox}$ gene, an essential Nox subunit gene, we also tested the role of Nox activation in podocyte EMT in vivo compared with their genetic background strain C57BL/6 mice.

Materials and methods

Cell culture Conditionally immortalized mouse podocyte cell line, kindly provided by Dr. Klotman PE (Division of Nephrology, Department of Medicine, Mount Sinai School of Medicine, New York, NY, USA), were cultured on collagen I-coated flasks or plates in RPMI 1640 medium supplemented with recombinant mouse interferon-γ at 33°C. After differentiation at 37°C for 10–14 days without interferon-γ, podocytes were used for the proposed experiments. In the present study, preparation of L-Hcys (a pathogenic form of Hcys), the concentration and incubation time of L-Hcys treatment were chosen based on our previous studies [50].

$gp91^{phox}$ siRNA transfection $gp91^{phox}$ siRNA was purchased from Qiagen, which was confirmed to be effective in silencing $gp91^{phox}$ gene in different cells by the company and had been successfully used in our previous studies [49]. The scrambled RNA (Qiagen, Valencia, CA, USA) was confirmed as non-silencing double-strand RNA and used as the control in the present study. Podocytes were serum-starved for 12 h and then transfected with $gp91^{phox}$ small interfering RNA (siRNA) or scrambled siRNA using siLentFect Lipid Reagent (Bio-Rad, Hercules, CA, USA). After 18 h of incubation at 37°C, the medium was changed, and L-Hcys (40 μmol/L) was added into the medium for indicated time span in different protocols.

Real-time reverse transcription polymerase chain reaction Total RNA from cultured podocytes or isolated mouse glomeruli was extracted using TRIzol reagent

(Invitrogen, Carlsbad, CA. USA) according to the protocol as described by the manufacturer. Aliquots of total RNA (1 μg) from each sample were reverse-transcribed into complementary DNA (cDNA) according to the instructions of the first strand cDNA synthesis kit manufacturer (Bio-Rad, Hercules, CA, USA). Equal amounts of the reverse transcriptional products were subjected to PCR amplification using SYBR Green as the fluorescence indicator on a Bio-Rad iCycler system (Bio-Rad, Hercules, CA, USA). The messenger RNA (mRNA) levels of target genes were normalized to the β-actin mRNA levels. The primers used in this study were synthesized by Operon (Huntsville, AL, USA), and the sequences were as follows: P-cadherin, sense GTAAGGGCTACCGCTCACTC and antisense TGTGAG GCCAAGTGAAAGAC; ZO-1, sense GAGCTACGCTTGC CACACTGT and antisense TCGGATCTCCAGGAAGACA CTT; FSP-1, sense GTTACCATGGCAAGACCCTT and antisense AACTTGTCACCCTCTTTGCC; α-SMA, sense CAGGATGCAGAAGGAGATCA and antisense TCCACAT CTGCTGGAAGGTA; β-actin, sense TCGCTGCGCTGGTC GTC and antisense GGCCTCGTCACCCACATAGGA.

Western blot analysis Western blot analysis was performed as we described previously [52]. In brief, proteins from the mouse glomeruli or cultured podocytes were extracted using sucrose buffer. After boiled for 5 min at 95°C in a 5× loading buffer, 50 μg of total proteins were subjected to sodium dodecyl sulfate polyacrylamide gel electrophoresis, transferred onto a polyvinylidene fluoride membrane and blocked. Then, the membrane was probed with primary antibodies of anti-gp91^{phox} (1:500, BD Biosciences, San Jose, CA, USA), anti-P-cadherin (1:200, R&D system, Minneapolis, MN, USA), anti-FSP-1 (1:500, Abcam, Cambridge, MA, USA), anti-α-SMA (1:200, R&D system, Minneapolis, MN, USA), or anti-β-actin (1:3,000, Santa Cruz Biotechnology, Santa Cruz, CA, USA) overnight at 4°C followed by incubation with horseradish peroxidase-labeled IgG (1:5,000). The immunoreactive bands were detected by chemiluminescence methods and visualized on Kodak Omat X-ray films. Densitometric analysis of the images obtained from X-ray films was performed using the Image J software (NIH, Bethesda, MD, USA).

Indirect immunofluorescent staining The cells were fixed in 4% paraformaldehyde (PFA) for 15 min. After rinsing with phosphate-buffered saline, cells were incubated with goat anti-FSP-1 (1:50, Abcam, Cambridge, MA, USA), goat anti-ZO-1 (1: 50, Santa Cruz Biotechnology, Inc, Santa Cruz, CA, USA), rabbit anti-P-cadherin (1: 50, R&D system, Minneapolis, MN, USA), and mouse anti-α-SMA (1: 100, R&D system, Minneapolis, MN, USA) antibodies. After washing, the slides were incubated with Alexa 488-labeled secondary antibodies for 1 h at room temperature. After being mounted with 4′,6-diamidino-2-phenylindole-containing mounting solution, the slides were observed under a fluorescence microscope, and photos were taken and analyzed. The fluorescent intensities were quantified by the Image Pro Plus 6.0 software (Media Cybernetics, Bethesda, MD, USA), and the data were normalized to control cells.

Cell permeability assay The permeability of podocyte monolayer was measured according to the methods as we described previously [43]. Briefly, cells were seeded in the upper chambers of 0.4 μm polycarbonate Transwell filters of a 24-well filtration microplate (Whatman Inc., Florham Park, NJ, USA). After treatment with L-Hcys (40 μmol/L) for different time spans or TGF-β1 (2.5 ng/ml) for 48 h, the culture medium was replaced with fresh phenol red-free RPMI 1640 in the presence of Hcys and 70 kD FITC-dextran (2.5 mol/l) in the upper chambers. After 4 h, the filtration microplate was removed, the medium from the lower compartment was collected, and then fluorescence was measured in a spectrofluorimeter at an excitation wavelength of 494 nm. The permeable fluorescence intensity was used to represent cell permeability, and the values were normalized to that of control cells.

Animal procedures C57BL/6J wild-type (WT; 8 weeks of age, male) and gp91^{phox} knockout (KO) mice (8 weeks of age, male) were bred from breeding pairs from The Jackson Laboratory, Bar Harbor, ME, USA. All protocols were approved by the Institutional Animal Care and Use Committee of Virginia Commonwealth University. To speed up the damaging effects of hHcys on glomeruli, all mice were uninephrectomized as described in previous studies [33, 45]. After a 1-week recovery period from the uninephrectomy, KO and WT mice were fed a normal diet or a folate-free (FF) diet (Dyets Inc, Bethlehem, PA, USA) for 4 weeks to induce hHcys. This model has been demonstrated to induce glomerular damage unrelated to the uninephrectomy and arterial blood pressure, but specific to hHcys [49]. One day before these mice were killed, 24-h urine samples were collected using mouse metabolic cages. After blood samples were collected, these mice were killed, and renal tissues were harvested for biochemical and molecular analysis as well as morphological examinations. Mouse glomeruli were isolated as described before [6]. Measurement of creatinine clearance (Ccr) was performed as we reported [49].

High performance liquid chromatography analysis Plasma total Hcys levels were measured by high performance liquid chromatography (HPLC) as we described previously [5]. Briefly, blood samples were centrifuged at 1,000×*g* for 10 min at 4°C to obtain plasma. A 100-μL plasma or

standard solution mixed with 10 μL of internal standard, thionglycolic acid (2.0 mmol/L) solution was treated with 10 μL of 10% tri-*n*-butylphosphine solution in dimethylformamide at 4°C for 30 min. Then, 80 μL of ice-cold 10% trichloroacetic acid in 1 mmol/L EDTA were added and centrifuged to remove proteins in the sample. One hundred microliters of the supernatant was transferred into the mixture of 20 μL of 1.55 mol/L sodium hydroxide, 250 μL of 0.125 mol/L borate buffer (pH 9.5), and 100 μL of 1.0 mg/mL ABD-F solution. The resulting mixture was incubated at 60°C for 30 min to accomplish derivatization of plasma thiols. HPLC was performed with an HP 1100 series equipped with a binary pump, a vacuum degasser, a thermostated column compartment, and an autosampler (Agilent Technologies, Waldbronn, Germany). Separation was carried out at an ambient temperature on an analytical column (Supelco LC-18-DB) with a Supelcosil LC-18 guard column. Fluorescence intensities were measured with an excitation wavelength of 385 nm and emission wavelength of 515 nm by a Hewlett-Packard Model 1046A fluorescence spectrophotometer. The peak area of chromatographs was quantified with a Hewlett-Packard 3392 integrator.

Electromagnetic spin resonance analysis of Nox-dependent $O_2^{\cdot-}$ production For the detection of Nox-dependent $O_2^{\cdot-}$ production, proteins from isolated glomeruli of mice or cultured podocytes were extracted using sucrose buffer (250 mmol/L sucrose, 20 mmol/L HEPES, 1 mmol/L EDTA, pH=7.4) and then re-suspended with modified Krebs–HEPES buffer containing deferoximine (100 μmol/L, Sigma, St. Louis, MO, USA) and diethyldithiocarbamate (5 μmol/L, Sigma, St. Louis, MO, USA). The Nox-dependent $O_2^{\cdot-}$ production was examined by the addition of 1 mmol/L NADPH as a substrate in 50 μg protein and incubated for 15 min at 37°C in the presence or absence of SOD (200 U/mL), and then supplied with 1 mM $O_2^{\cdot-}$ specific spin trap 1-hydroxy-3-methoxycarbonyl-2,2,5,5-tetramethylpyrrolidine (Noxygen, Elzach, Germany) as we described previously [45]. The mixture was loaded in glass capillaries and immediately analyzed for $O_2^{\cdot-}$ production kinetically for 10 min in a Miniscope MS200 electromagnetic spin resonance (ESR) spectrometer (Magnettech Ltd, Berlin, Germany). The ESR settings were as follows: biofield, 3,350; field sweep, 60 G; microwave frequency, 9.78 GHz; microwave power, 20 mW; modulation amplitude, 3 G; 4,096 points of resolution; and receiver gain, 20 for tissue and 50 for cells. The results were expressed as the fold changes of control.

Urinary albumin excretion measurement The 24-h urine albumin was detected using a commercially available mouse albumin ELISA kit (Bethyl Laboratories, Montgomery, TX, USA) as we described previously [49].

Morphological examination For observation of renal morphology using light microscope, pre-fixation perfusion using phosphate buffer was done prior to fixation to ensure removal of blood. The kidneys were then perfused using 4% PFA in situ, and renal tissues were post-fixed, paraffin-embedded, and stained with periodic acid–Schiff (PAS). Then, glomerular pathological changes were assessed by an observer blinded to the study. Glomerular damage was assessed by a standard semi-quantitative analysis and expressed as glomerular damage index (GDI) as we described before [13]. Fifty glomeruli per slide were counted and graded as 0, 1, 2, 3, or 4, according to 0, <25, 25–50, 51–75, or >75% glomerular damage across a longitudinal kidney section, respectively. The GDI for each mouse was calculated by the formula: $(N_1\times1+N_2\times2+N_3\times3+N_4\times4)/n$, where N_1, N_2, N_3, and N_4 represent the numbers of glomeruli exhibiting grades 1, 2, 3, and 4, respectively, and n is the total number of glomeruli graded.

For transmission electron microscopic (TEM) observation of ultrastructural changes in podocytes, the kidneys were perfused with a fixative containing 3% glutaraldehyde and 4% paraformaldehyde in 0.1 mol/L phosphate buffer. After fixation and dehydration with ethanol, the samples were embedded in Durcupan resin for ultra-thin sectioning and TEM examinations by VCU electron microscopy core facility.

Double-immunofluorescent staining Double-immunofluorescent staining was performed using frozen slides from mouse kidneys. After fixation, the slides were incubated with rabbit anti-podocin 1: 200 (Sigma, St. Louis, MO, USA), which was followed by incubation with Alexa 555-labeled goat anti-rabbit secondary antibody. Then, goat anti-FSP-1 (1:50, Abcam, Cambridge, MA, USA), goat anti-ZO-1 1:50 (Santa Cruz Biotechnology Inc, Santa Cruz, CA, USA), rabbit anti-P-cadherin 1:100 (R&D system, Minneapolis, MN, USA), or mouse anti-α-SMA 1:200 (R&D system, Minneapolis, MN, USA) was used to incubate the slides for overnight at 4°C. After washing, the slides were incubated with Alexa 488-labeled secondary antibodies. Finally, the slides were mounted and subjected to examinations using a confocal laser scanning microscope (Fluoview FV1000, Olympus, Japan).

Statistical analysis All of the values are expressed as mean±SEM. Significant differences among multiple groups were examined using ANOVA followed by a Student–Newman–Keuls test. χ^2 test for testing the significance of ratio and percentage data. $P<0.05$ was considered statistically significant.

Results

L-Hcys suppressed epithelial P-cadherin and ZO-1 expression in podocytes We first examined the expression of P-cadherin, an epithelial marker, in podocytes before and after Hcys treatment. As shown in Fig. 1a, treatment of podocytes with Hcys markedly suppressed P-cadherin mRNA expression in a concentration-dependent manner as detected by real-time reverse transcription PCR (RT-PCR). P-cadherin mRNA expression started to decrease after treatment with 20 μmol/L of L-Hcys for 48 h, and L-Hcys at a concentration of 40 or 80 μmol/L could further decrease P-cadherin mRNA expression in podocytes, which was almost comparable to a well-established EMT inducer, TGF-β1 (2.5 ng/ml) [15, 20]. Immunofluorescence staining (Fig. 1b) further showed that P-cadherin protein expression was substantially reduced by treatment of podocytes with L-Hcys (40 μmol/L) for 72 h. In consistent with these data, L-Hcys-induced P-cadherin suppression was also confirmed by Western blot analysis (Figure S1A).

ZO-1 is a tight junction-associated protein, which is located at the slit diaphragm and is linked to nephrin [29]. This protein is also widely used as an epithelial marker for podocytes. In the present study, real-time RT-PCR data showed that ZO-1 mRNA expression was decreased by the treatment with L-Hcys, with the strongest effect at a concentration of 40 μmol/L (Fig. 1c). Immunofluorescence staining showed abundant ZO-1 at the sites of cell–cell contacts with a characteristic zipper-like pattern between interdigitating processes of podocytes. Interestingly, the overall density of ZO-1 staining was markedly decreased in L-Hcys-treated cells, which was similar to that induced by TGF-β1 (Fig. 1d).

L-Hcys increased the expression of mesenchymal markers in podocytes We next investigated whether L-Hcys could induce a mesenchymal transition of podocytes. To this end, the expression of two mesenchymal markers, FSP-1 and α-SMA, were examined in podocytes after L-Hcys treatment. As illustrated in Fig. 2a and c, incubation of these cells with L-Hcys induced the expression of FSP-1 and α-SMA mRNA in a dose-dependent manner, which was similar to the effect of TGF-β1. Immunostaining showed that podocytes under basal conditions barely expressed FSP-1 and α-SMA. However, after stimulated by L-Hcys (40 μmol/L) for 72 h, there were clearly increased FSP-1 and α-SMA expression in the cytoplasm of these cells (Fig. 2b, d), indicating that mesenchymal characteristics of podocytes were obtained under Hcys stimulation. Western blot analysis showed that α-SMA expression was significantly increased upon the stimulation of L-Hcys, although it is less potent as the classic EMT inducer, TGF-β1 (Figure S1B).

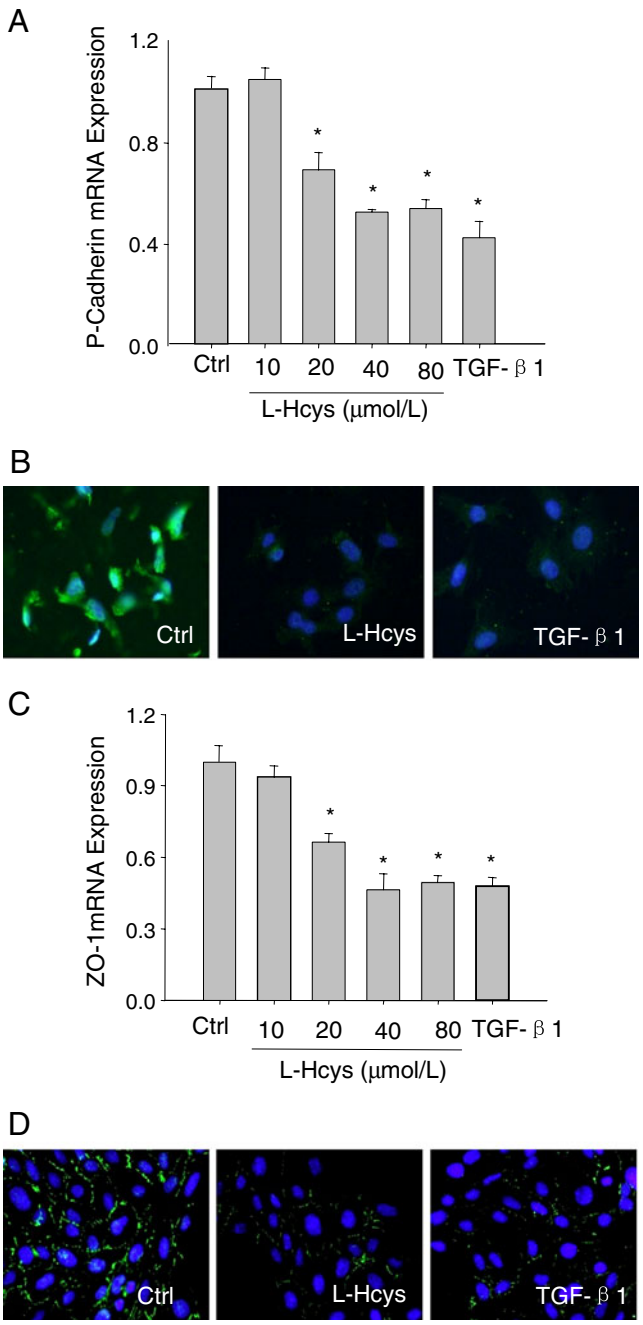

Fig. 1 L-Hcys suppressed epithelial P-cadherin and ZO-1 expression in podocytes. Podocytes were stimulated with different concentrations of L-Hcys or TGF-β1 (2.5 ng/mL) for 48 h. The mRNA level of P-cadherin (**a**) and ZO-1 (**c**) were detected using real-time RT-PCR (n=6) per group. *P<0.05 vs. Ctrl. Immunofluorescence staining shows the expression of P-cadherin (**b**) and ZO-1 (**d**) in control cells or cells treated with L-Hcys (40 μM) or TGF-β1 (2.5 ng/mL) for 72 h. Original magnification, ×400. Images are representative of five batches of cells for each group

Dependency of Hcys-induced phenotype changes on O_2^- production via Nox activation in podocytes To explore the mechanism mediating Hcys-induced EMT, we performed

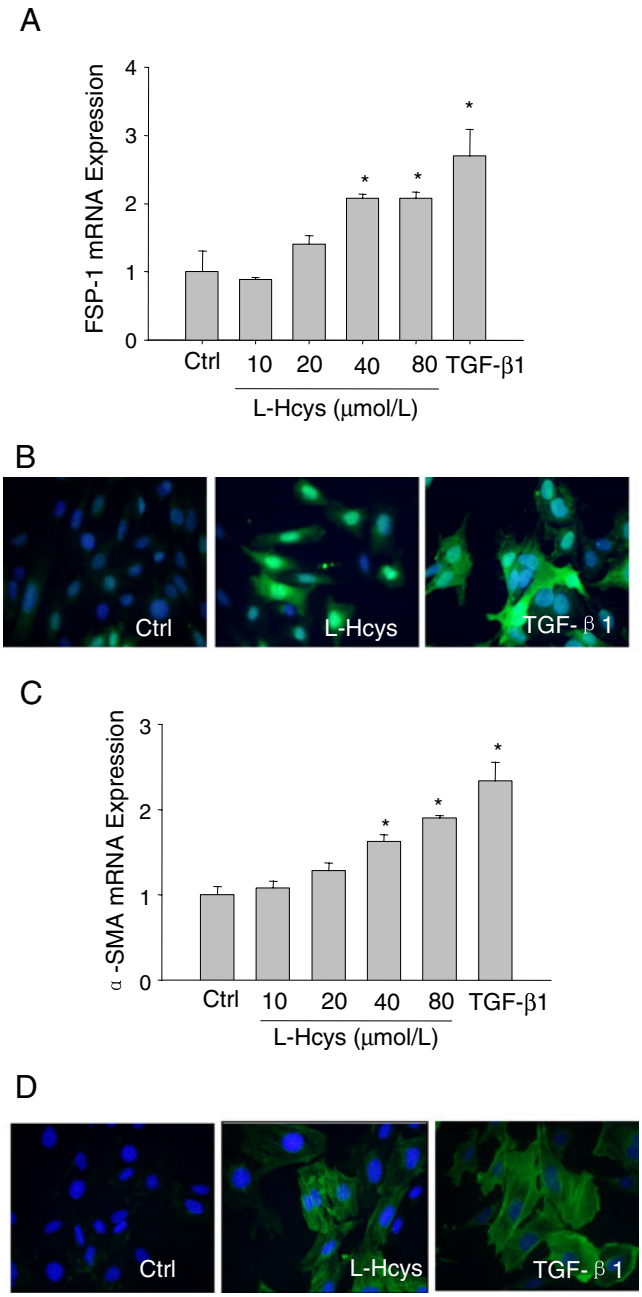

Fig. 2 L-Hcys induced mesenchymal marker expression in podocytes. Podocytes were stimulated with different concentrations of L-Hcys or TGF-β1 (2.5 ng/mL) for 48 h. The mRNA level of FSP-1 (**a**) and α-SMA (**c**) were detected using real-time RT-PCR (n=6 per group). *P<0.05 vs. Ctrl. Immunofluorescence staining shows the expression of FSP-1 (**b**) and α-SMA (**d**) in control cells or cells treated with L-Hcys (40 μM) or TGF-β1 (2.5 ng/ml)for 72 h. Original magnification, ×400. Images are representative of five batches of cells for each group

experiments to measure L-Hcys-induced Nox-dependent $O_2^{\cdot-}$ production. In consistent with our previous data [49], with a 48-h incubation L-Hcys concentration-dependently increased Nox-dependent $O_2^{\cdot-}$ production with a maximal increase of 2.38±0.30-fold at 40 μmol/L of Hcys, as compared with control cells (P<0.05, n=5). When podocytes were transfected with gp91^{phox} siRNA, Hcys-induced gp91^{phox} protein expression was substantially inhibited (Figure S2), suggesting a successful knocking down of this gene. Under these conditions, Nox-dependent $O_2^{\cdot-}$ production induced by L-Hcys was also significantly inhibited (1.10±0.22 vs. 2.27±0.27-fold as compared with control cells, P<0.05, n=4), indicating that $O_2^{\cdot-}$ production in podocytes is mainly derived from the activation of Nox.

Consistent with direct measurement of $O_2^{\cdot-}$ production under different treatments, gp91^{phox} siRNA was found to block Hcys-induced decreases in P-cadherin and ZO-1 expression in podocytes compared to that observed in vehicle- or scrambled siRNA-treated cells. Similarly, inhibition of Nox activity using DPI or apocynin also prevented the loss of these epithelial markers in podocytes (Fig. 3a, two left groups of images). Correspondingly, the mesenchymal transition of podocytes, namely, increase in FSP-1 expression induced by Hcys, was also abolished by gp91^{phox} siRNA transfection or by DPI or apocynin, indicating preservation of epithelial phenotype of podocytes. Additionally, inhibition of Nox also dramatically attenuated Hcys-induced α-SMA expression in podocytes treated with L-Hcys (Fig. 3a, two right groups of images). Relative fluorescent intensities of these markers are summarized in Fig. 3b.

Inhibition of EMT improved barrier function of podocytes We next examined whether podocyte EMT associated with $O_2^{\cdot-}$ production affects the barrier function of podocyte monolayer. Dextran flux assay was used to assess the filtration across the monolayer of cultured differentiated podocytes. As shown in Fig. 4a, increased dextran flux was observed in podocytes treated with L-Hcys for 48 or 72 h, when compared with control cells (P<0.05). As expected, TGF-β1 also induced a significant increase in cell permeability in the podocyte monolayer after 48 h of incubation, which was used as a positive control for this assay. Inhibition of Nox activity using its inhibitors (DPI and apocynin) or gp91 siRNA significantly recovered podocyte permeability (P<0.05, Fig. 4b).

Expression of epithelial and mesenchymal markers in glomeruli of WT mice on the FF diet HPLC analysis showed that both strains of mice had higher plasma homocysteine levels on FF diet compared to the mice on normal diet (Table 1). Real-time RT-PCR data showed that hHcys induced by the FF diet significantly decreased the mRNA levels of two important epithelial markers, P-cadherin and ZO-1, in the glomeruli isolated from WT mouse kidneys, but it had no significant effect on the expression of these epithelial markers in glomeruli from gp91^{phox} KO mice (Fig. 5a, b). The protein expression of P-cadherin was also found to be much lower in WT mice on the FF diet but not KO mice on

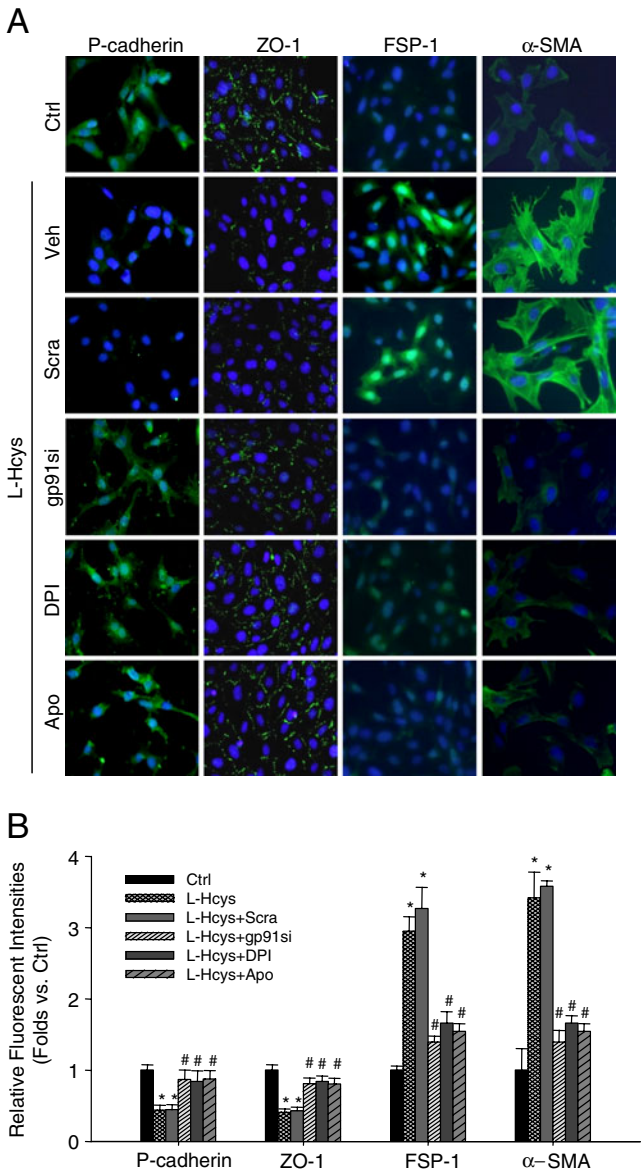

Fig. 3 Reversal of EMT in Hcys-treated podocytes by inhibition of Nox. **a** Immunofluorescence staining showed that inhibition of Nox activation by gp91^{phox} siRNA, DPI, or apocynin rescued Hcys-induced loss of epithelial markers, P-cadherin and ZO-1. Inhibition of Nox activation also resulted in suppressed expression of mesenchymal markers, FSP-1 and α-SMA. Images are representative of five batches of cells for each group. Original magnification, ×400. **b** Summarized data shows relative fluorescent intensities of P-cadherin, ZO-1, FSP-1, and α-SMA. *Ctrl* Ctrl; *Veh* vehicle; *Scra* scrambled siRNA; *gp91si* gp91^{phox} siRNA; *Apo* apocynin. n=5 batches of cells. *P<0.05 vs. Ctrl, $^{\#}P$<0.05 vs. L-Hcys

the same treatment (Fig. 6a). However, the mRNA expression of FSP-1 and α-SMA, two mesenchymal markers, were markedly increased in WT mice as compared with gp91^{phox} KO mice when these animals suffered from hHcys (P<0.05, Fig. 5c, d). In consistent with the changes on mRNA level, the protein expression of FSP-1 and α-SMA in mouse glomeruli was dramatically induced by hHcys in WT mice, which was much lower in KO mice (Fig. 6b, c). Accompanied with these cellular functional changes, hHcys significantly increased glomerular $O_2^{\cdot-}$ production in WT mice, but not in KO mice (1.39±0.26 vs. 2.80±0.30-fold increases, P<0.05, n=5).

Attenuation of hHcys-associated podocyte EMT in gp91^{phox} gene KO mice To further confirm podocyte phenotypic changes during hHcys and the role of Nox activation in this process, fluorescence double-immunostaining was performed using podocin as a podocyte marker. As shown in Fig. 7a, podocin staining was shown as a fine linear-like pattern along the glomerular capillary loop in mice on a normal diet (WT-ND), which was largely colocalized with P-cadherin. When mice were exposed to the FF diet, the expression of both podocin and P-cadherin showed a dramatic decrease in WT mice (WT-FF) but only a much slighter decrease in gp91^{phox} KO mice (KO-FF). Similar staining pattern was found for the colocalization of ZO-1

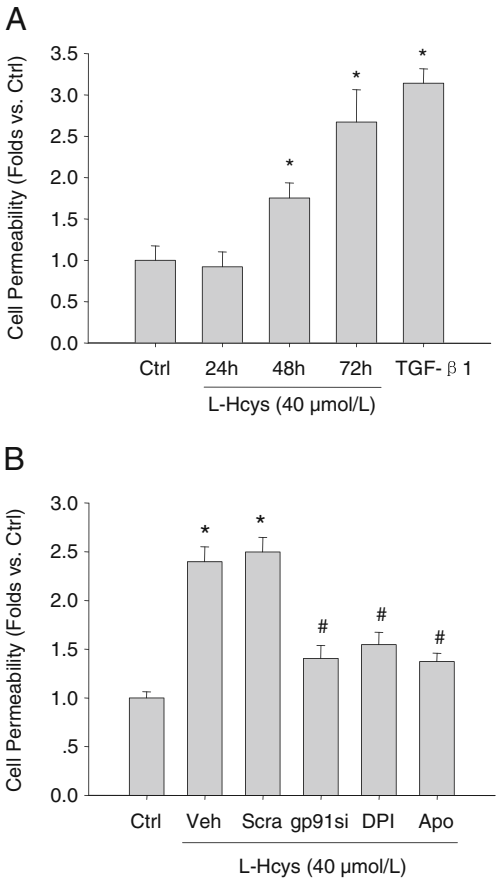

Fig. 4 Effect of Nox inhibition on Hcys-induced enhancement of podocyte monolayer permeability. **a** L-Hcys induced an increase of podocyte monolayer permeability in a time-dependent manner. **b** Effects of Nox inhibition on Hcys-induced enhancement of podocyte monolayer permeability after 72 h. *Ctrl* control; *Veh* vehicle; *Scra* scrambled siRNA; *gp91si* gp91^{phox} siRNA; *Apo* apocynin. n=5 per group. *P<0.05 vs. Ctrl, $^{\#}P$<0.05 vs. L-Hcys

Table 1 Plasma total Hcys, urine albumin, creatinine clearance, and glomerular damage index data in WT or gp91^{phox} KO mice fed with normal diet or FF diet

Parameter	WT-ND, n=10	KO-ND, n=7	WT-FF, n=11	KO-FF, n=8
Total Hcys (μmol/L)	4.25±0.54	4.61±0.77	15.56±1.76*	14.66±2.02*
Urine albumin (μg/24 h)	13.21±0.82	15.63±4.37	41.59±4.58*	23.61+2.36**
Ccr (μl/min)	76.09±5.43	74.60±4.80	50.36±2.28*	67.03±5.06**
GDI	0.70±0.15	0.80±0.13	2.80±0.36*	1.30±0.15**

The data is expressed as mean±SEM

ND Normal diet; *FF* FF diet; *Ccr* creatinine clearance; *GDI* glomerular damage index

*p<0.05 as compared with WT-ND; **p<0.05 as compared with WT-FF

and podocin (Fig. 7a, right images). As shown in Fig. 7b, although FSP-1 and α-SMA expressions were weak in the glomeruli of WT mice on the normal diet (WT-ND), it was dramatically increased in the glomeruli of these mice on the FF diet (WT-FF), which showed a large degree of colocalization with podocin. However, the expression of these two mesenchymal markers were substantially decreased in podocytes in the KO mice on the same diet (KO-FF), as demonstrated by lower levels of expression and less colocalization with podocin (Fig. 7b).

Alleviation of hHcys-induced glomerular injury in gp91^{phox} KO mice As shown in Fig. 8a, PAS staining detected marked glomerular sclerotic damages in WT mice on the FF diet, as featured by significant mesangial expansion, glomerular capillary collapse, and fibrosis. In gp91^{phox} gene KO mice, these sclerotic changes in glomeruli were significantly suppressed. The average GDI was substantially higher in WT mice compared to gp91^{phox} KO mice on the FF diet (P<0.05, Table 1). To evaluate the ultrastructural changes of podocytes, TEM experiments were conducted. Compared with the distinct brush-like structures of podocyte foot processes in mice on the normal diet, evident foot process effacement was observed in WT mice after FF diet treatment. In contrast, podocytes of gp91^{phox} KO mice on the FF diet had relatively normal ultrastructures (Fig. 8b).

Urinary albumin excretion, moreover, as a parameter for podocyte barrier function and glomerular damage, was found to be significantly increased in WT mice on the FF diet, but this increase in urinary albumin excretion was not detected in gp91^{phox} KO mice (P<0.05, Table 1). To evaluate the glomerular filtration rate, Ccr was measured. It was found that FF diet treatment induced a decline in Ccr in WT mice, whereas the Ccr was mostly preserved in gp91^{phox} KO mice on the FF diet (P<0.05, Table 1).

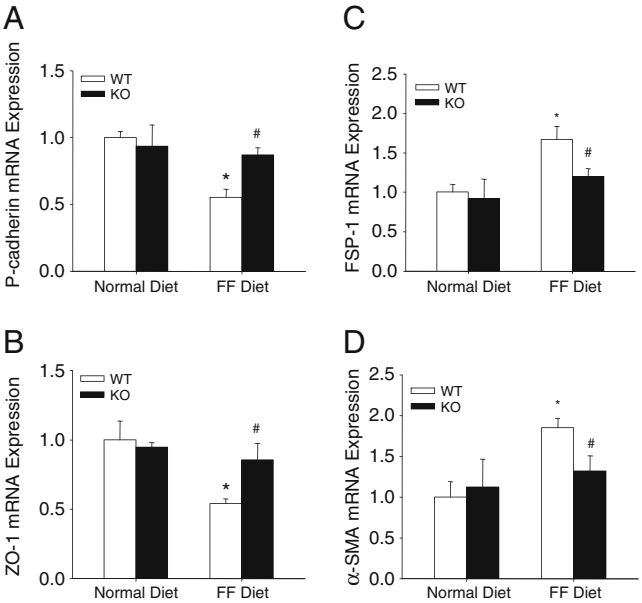

Fig. 5 Expression of the mRNA of epithelial and mesenchymal markers in the glomeruli isolated from gp91^{phox} KO and WT mice. **a**, **b** Real-time RT-PCR analysis for the expression of epithelial markers (P-cadherin and ZO-1) in the glomeruli of gp91 KO and WT mice (n=4 per group). **c**, **d** Relative mRNA expression of mesenchymal markers (FSP-1 and α-SMA) in the glomeruli of gp91 KO and WT mice (n=4 per group). *P<0.05 vs. WT mice on the normal diet; #P<0.05 vs. WT mice on the FF diet

Discussion

The major goal of this study was to determine whether podocytes could undergo phenotypic changes and thereby lead to glomerular injury during hHcys and to address whether Nox-dependent $O_2^{\cdot-}$ production is involved in this process. Using in vitro cultured podocytes and a FF diet-induced hHcys animal model in gp91^{phox} gene KO mice, we provided reliable evidence that hHcys directly induced podocyte EMT, podocyte dysfunction, and consequently glomerular damage through gp91^{phox}-containing Nox activation and $O_2^{\cdot-}$ production.

The EMT is referred to as the process of cell transition from epithelial to mesenchymal phenotype, which usually happens during normal developmental process, cancer

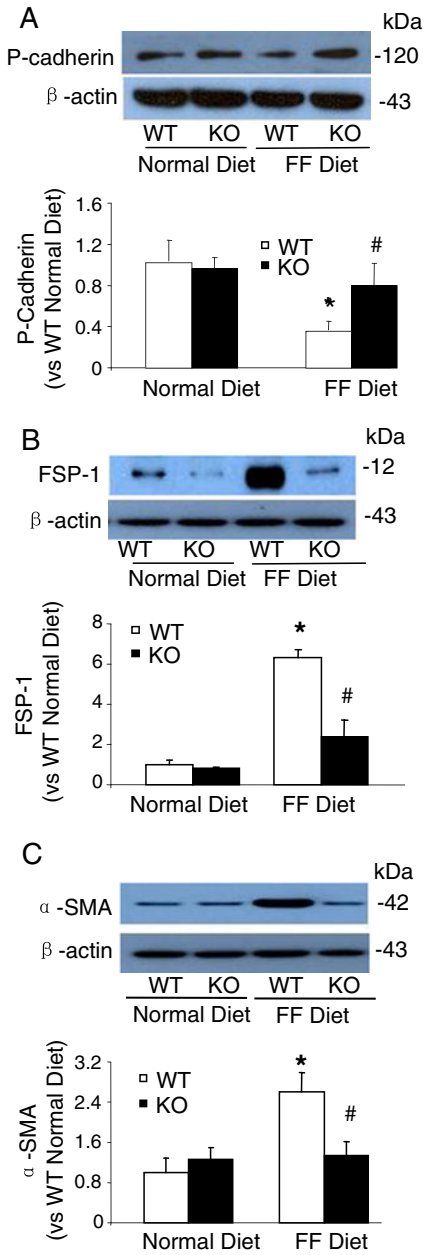

Fig. 6 Western blot analysis of P-cadherin, FSP-1, and α-SMA protein expression in mouse glomeruli. **a** A representative gel image (*upper panel*) shows the expression of P-cadherin in mouse glomeruli from different group of mice as indicated and the relative quantization of P-cadherin protein expression was summarized (*lower panel*). **b** A representative gel image (*upper panel*) shows the expression of FSP-1 in mouse glomeruli from different group of mice as indicated, and the relative quantization of FSP-1 protein expression was summarized in the *lower panel*. **c** A representative gel image (*upper panel*) shows the expression of α-SMA in mouse glomeruli from different group of mice as indicated, and the relative quantization of α-SMA protein expression was summarized in the lower panel. $n=4$.*$P<0.05$ vs. WT mice on the normal diet; $^{\#}P<0.05$ vs. WT mice on the FF diet

progression, and metastasis [1]. In the kidney, the EMT process was well documented in tubular epithelial cells in the development of tubulo-interstitial fibrosis [38], where injured proximal or distal tubular epithelial cells could undergo dramatic phenotypic changes, such as the loss of epithelial markers (E-cadherin and cytokeratin) along with the acquisition of some mesenchymal marker (such as α-SMA), being accompanied by related function changes. These transformed cells (i.e., myofibroblasts) have been demonstrated to participate in the initiation and progression of tubulo-interstitial fibrosis by migrating into the interstitial area to produce abnormal extracellular matrix [7]. Given that podocytes and tubular epithelial cells are developmentally derived from the same origin (metanephric mesenchyme) [19], it is possible that podocytes, similar to tubular epithelial cells, may undergo a phenotypic conversion under specific injurious conditions. Indeed, some recent studies reported that podocytes could undergo phenotypic change under some pathological conditions, such as diabetic nephropathy [15, 20], focal segmental glomerulosclerosis [27], and HIV-associated nephropathy [22], although this transition of podocyte is not regarded as classic EMT like in cancer genesis. These studies highlighted the possible involvement of podocyte phenotypic changes in the pathogenesis of proteinuric diseases; however, its role in hHcys-induced podocytes injury and related mechanism activating EMT remain unclear.

In the present study, we first used in vitro cultured podocytes to investigate the possible effects of Hcys on podocyte phenotype changes. Our results showed that the epithelial markers, P-cadherin and ZO-1, were decreasingly expressed in podocytes when podocytes were treated with different concentrations of L-Hcys, indicating the loss of their epithelial characteristics. It was also found that such loss of podocyte epithelial features after L-Hcys stimulation was accompanied by induction of mesenchymal markers, namely, increases in FSP-1 and α-SMA expression, further suggesting the EMT of podocytes in response to Hcys. To our knowledge, this is the first report demonstrating that renal residential cells could undergo EMT under the stimulation of Hcys. In consistent with our findings, a recent study by Sen *et al.* has shown that Hcys-mediated TGF-β1 up-regulation triggers endothelial-myofibroblast differentiation in mouse aortic endothelial cells, which was involved in ECM remodeling and participated in vascular thickening and stiffness [34]. In terms of podocyte EMT, recent studies have demonstrated that podocytes could trans-differentiate into myofibroblasts under different stimulators such as TGF-β1, adriamycin, and high glucose [15].

Next, we explored the possible mechanisms involving in Hcys-induced podocyte EMT process. Since our previous studies demonstrated that Hcys significantly induces Nox activation, resulting in $O_2^{\cdot-}$ production, which was considered as a very early mechanism mediating Hcys-induced glomerular injury [43, 46, 50], we wonder whether podocyte EMT is associated with Nox activation. It was indeed found that L-

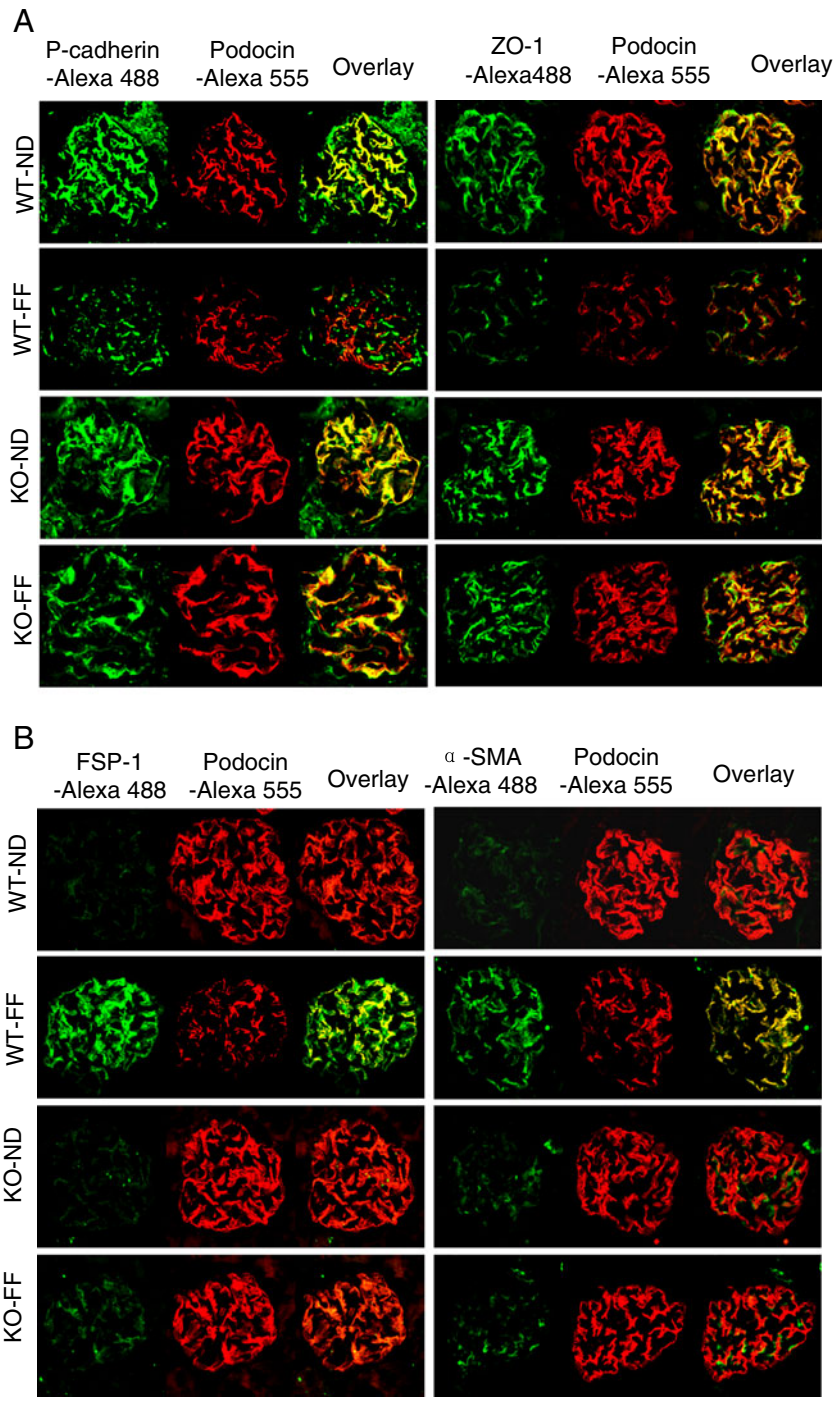

Fig. 7 Podocyte EMT was attenuated in mice lacking gp91^{phox} gene. **a** Frozen kidney sections from WT or gp91phox KO mice were double-immunostained for P-cadherin or ZO-1 (Alexa 488, *green color*) and podocyte marker podocin (Alexa 555, *red color*). **b** Mouse kidney sections were double-immunostained for mesenchymal markers FSP-1 or α-SMA (Alexa 488, *green color*) and podocin (Alexa 555, *red color*). n=6 per group

Hcys stimulation for 48 h induced a significant increase in Nox-dependent $O_2^{\cdot-}$ production in these cells and inhibition of Nox activity or silencing gp91^{phox} gene, a membrane Nox subunit, substantially blocked L-Hcys-induced loss of epithelial markers in podocytes and inhibited the conversion of these cells into mesenchymal phenotype. These data suggest that Hcys-induced EMT in vitro is mediated by the activation of Nox and subsequent generation of reactive oxygen species (ROS). In support of our findings, accumulating evidence shows that ROS, including Nox-dependent $O_2^{\cdot-}$, play a central role in mediating the EMT process such as findings in cancer cells [39], lung mesenchymal cells [12], alveolar epithelial cells [9], and renal tubular epithelial cells [30].

To address the functional relevance of Hcys-induced EMT, the barrier function of podocytes as the final defense in preventing protein leakage from the plasma into urine [4,

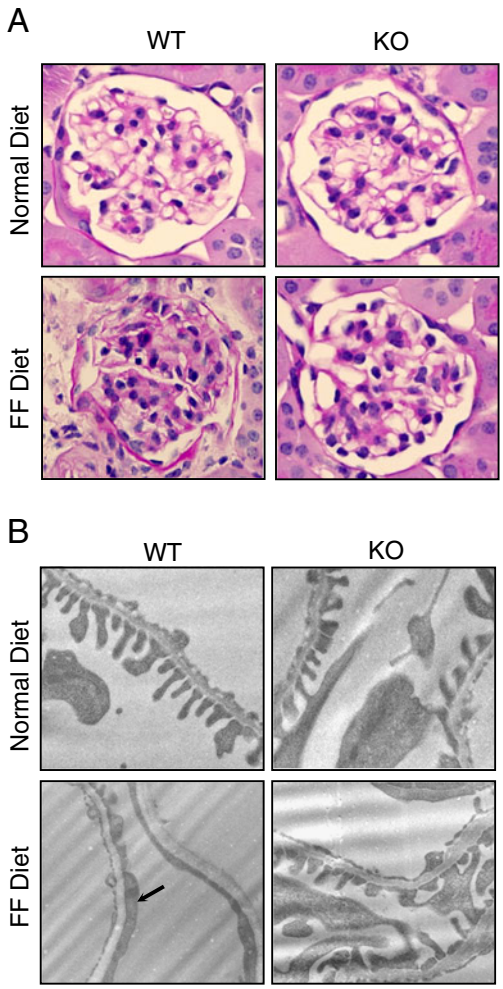

Fig. 8 Protection of podocytes and glomeruli from hHcys-induced injury in gp91^{phox} KO mice. **a** PAS staining shows glomerular morphological changes (original magnification, ×400). **b** gp91^{phox} gene deletion improved podocyte ultrastructure in FF diet-treated mice as shown by TEM examination. *Arrow* denotes the area of foot process effacement in WT mice on the FF diet. Images are representative of five TEM images per kidney from three mice per group. Original magnification, ×8,000

36, 51] was examined. We found that treatment of podocytes with L-Hcys significantly increased dextran influx across trans-differentiated podocytes, which was restored by inhibition of Nox, indicating that podocyte barrier function was severely impaired after the phenotypic conversion mediated by Nox activation. Using an albumin influx system, a recent report also recorded a similar effect of TGF-β-induced impairment on podocyte permeability through the induction of podocyte EMT, although the role of Nox was not addressed in that study [20]. From these results, a conclusion can be drawn that L-Hcys is sufficient to cause podocyte phenotype altercations via Nox activation, and this phenotypic change in podocytes is attributed to impaired filtration barrier function.

To further support this view, we used gp91^{phox} KO mice and their genetic background strain to determine the role of Nox-mediated $O_2^{\cdot-}$ production in hHcys-induced podocyte EMT and its functional relevance in vivo. gp91^{phox}, also known as NOX2, is the catalytic subunit of Nox. Data from our laboratory and by other groups have strongly suggested that the gp91^{phox}-containing Nox system is essential in mediating $O_2^{\cdot-}$ production in the kidney in response to hHcys or other stimuli [10, 11, 44, 46]. In the present study, it was found that the FF diet treatment increased plasma Hcys levels in both WT and KO mice, indicating a successful establishment of hHcys mouse model, and also suggests that gp91^{phox} itself is not involved in the metabolism of Hcys. gp91^{phox} KO mice on the FF diet exhibited lower levels of glomerular $O_2^{\cdot-}$ production compared with WT mice, implying that gp91^{phox} gene deficiency prevents hHcys-induced local $O_2^{\cdot-}$ production in glomeruli.

One of the most important findings of the present study is that gp91^{phox} gene deficiency may protect podocytes from hHcys-induced EMT, which was supported by restoration of some epithelial markers (such as P-cadherin and ZO-1) and attenuated expression of the mesenchymal markers (such as FSP-1 and α-SMA) in the glomeruli isolated from these mice. These data clearly demonstrate the occurrence of podocyte EMT during hHcys, which results from Nox-derived ROS generation locally in the kidney. In accordance with alleviated podocyte EMT in gp91^{phox} KO mice on the FF diet, urine albumin excretion in these mice was significantly decreased as compared with WT mice on the same diet, suggesting that podocyte barrier function is improved in these KO mice. Additionally, our pathological studies showed that there was a significant improvement of hHcys-induced glomerular damage and foot process effacement in these KO mice. In concert, the results from these in vivo experiments further support the view that Nox-mediated ROS generation is critically involved in mediating podocyte EMT and consequent glomerular functional impairment.

In summary, we demonstrated that Hcys directly induced podocytes to undergo EMT process through the activation of Nox in vitro, which resulted in damaged podocyte barrier function. The amelioration of podocyte EMT in gp91^{phox} KO mice during hHcys further strengthened the conclusion that Nox activation plays an important role in mediating hHcys-induced podocyte EMT and initiating glomerulosclerosis. The findings presented in this study reveal podocyte EMT as a novel mechanism initiating hHcys-induced podocyte injury and consequent glomerulosclerosis during hHcys and thereby direct the development of potential new therapeutic strategies for treatment and prevention of glomerulosclerosis associated with hHcys.

Acknowledgments This work was supported by grants DK54927, HL075316, and HL57244 from National Institutes of Health to Dr. Pin-Lan Li and a grant from National Natural Science Foundation of China (31050110433) to Dr. Krishna M. Boini.

Conflict of interest statement No conflicts of interest, financial or otherwise are declared by the authors.

References

1. Acloque H, Adams MS, Fishwick K, Bronner-Fraser M, Nieto MA (2009) Epithelial–mesenchymal transitions: the importance of changing cell state in development and disease. J Clin Invest 119:1438–1449
2. Appel D, Kershaw DB, Smeets B, Yuan G, Fuss A, Frye B, Elger M, Kriz W, Floege J, Moeller MJ (2009) Recruitment of podocytes from glomerular parietal epithelial cells. J Am Soc Nephrol 20:333–343
3. Bariety J, Hill GS, Mandet C, Irinopoulou T, Jacquot C, Meyrier A, Bruneval P (2003) Glomerular epithelial–mesenchymal transdifferentiation in pauci-immune crescentic glomerulonephritis. Nephrol Dial Transplant 18:1777–1784
4. Chen S, Fang Z, Zhu Z, Deng A, Liu J, Zhang C (2009) Protective effect of sulodexide on podocyte injury in adriamycin nephropathy rats. J Huazhong Univ Sci Technolog Med Sci 29:715–719
5. Chen YF, Li PL, Zou AP (2002) Effect of hyperhomocysteinemia on plasma or tissue adenosine levels and renal function. Circulation 106:1275–1281
6. Dai C, Stolz DB, Bastacky SI, St-Arnaud R, Wu C, Dedhar S, Liu Y (2006) Essential role of integrin-linked kinase in podocyte biology: bridging the integrin and slit diaphragm signaling. J Am Soc Nephrol 17:2164–2175
7. Deng B, Yang X, Liu J, He F, Zhu Z, Zhang C (2010) Focal adhesion kinase mediates TGF-beta1-induced renal tubular epithelial-to-mesenchymal transition in vitro. Mol Cell Biochem 340:21–29
8. Ducloux D, Motte G, Challier B, Gibey R, Chalopin JM (2000) Serum total homocysteine and cardiovascular disease occurrence in chronic, stable renal transplant recipients: a prospective study. J Am Soc Nephrol 11:134–137
9. Felton VM, Borok Z, Willis BC (2009) N-Acetylcysteine inhibits alveolar epithelial–mesenchymal transition. Am J Physiol Lung Cell Mol Physiol 297:L805–L812
10. Haque MZ, Majid DS (2004) Assessment of renal functional phenotype in mice lacking gp91PHOX subunit of NAD(P)H oxidase. Hypertension 43:335–340
11. Haque MZ, Majid DS (2008) Reduced renal responses to nitric oxide synthase inhibition in mice lacking the gene for gp91phox subunit of NAD(P)H oxidase. Am J Physiol Renal Physiol 295:F758–F764
12. Hecker L, Vittal R, Jones T, Jagirdar R, Luckhardt TR, Horowitz JC, Pennathur S, Martinez FJ, Thannickal VJ (2009) NADPH oxidase-4 mediates myofibroblast activation and fibrogenic responses to lung injury. Nat Med 15:1077–1081
13. Iacobini C, Menini S, Oddi G, Ricci C, Amadio L, Pricci F, Olivieri A, Sorcini M, Di Mario U, Pesce C, Pugliese G (2004) Galectin-3/AGE-receptor 3 knockout mice show accelerated AGE-induced glomerular injury: evidence for a protective role of galectin-3 as an AGE receptor. FASEB J 18:1773–1775
14. Ingram AJ, Krepinsky JC, James L, Austin RC, Tang D, Salapatek AM, Thai K, Scholey JW (2004) Activation of mesangial cell MAPK in response to homocysteine. Kidney Int 66:733–745
15. Kang YS, Li Y, Dai C, Kiss LP, Wu C, Liu Y (2010) Inhibition of integrin-linked kinase blocks podocyte epithelial-mesenchymal transition and ameliorates proteinuria. Kidney Int 78:363–373
16. Kriz W (2003) Progression of chronic renal failure in focal segmental glomerulosclerosis: consequence of podocyte damage or of tubulointerstitial fibrosis? Pediatr Nephrol 18:617–622
17. Kriz W (2007) Ontogenetic development of the filtration barrier. Nephron Exp Nephrol 106:e44–e50
18. Kriz W, Kaissling B, Le Hir M (2011) Epithelial–mesenchymal transition (EMT) in kidney fibrosis: fact or fantasy? J Clin Invest 121:468–474
19. Lehtonen S, Tienari J, Londesborough A, Pirvola U, Ora A, Reima I, Lehtonen E (2008) CD2-associated protein is widely expressed and differentially regulated during embryonic development. Differentiation 76:506–517
20. Li Y, Kang YS, Dai C, Kiss LP, Wen X, Liu Y (2008) Epithelial-to-mesenchymal transition is a potential pathway leading to podocyte dysfunction and proteinuria. Am J Pathol 172:299–308
21. Liu Y (2010) New insights into epithelial-mesenchymal transition in kidney fibrosis. J Am Soc Nephrol 21:212–222
22. Lu TC, He JC, Klotman PE (2007) Podocytes in HIV-associated nephropathy. Nephron Clin Pract 106:c67–c71
23. Matsui I, Hamano T, Tomida K, Inoue K, Takabatake Y, Nagasawa Y, Kawada N, Ito T, Kawachi H, Rakugi H, Imai E, Isaka Y (2009) Active vitamin D and its analogue, 22-oxacalcitriol, ameliorate puromycin aminonucleoside-induced nephrosis in rats. Nephrol Dial Transplant 24:2354–2361
24. Moustapha A, Gupta A, Robinson K, Arheart K, Jacobsen DW, Schreiber MJ, Dennis VW (1999) Prevalence and determinants of hyperhomocysteinemia in hemodialysis and peritoneal dialysis. Kidney Int 55:1470–1475
25. Mundel P (2003) Urinary podocytes: lost and found alive. Kidney Int 64:1529–1530
26. Nagase M, Yoshida S, Shibata S, Nagase T, Gotoda T, Ando K, Fujita T (2006) Enhanced aldosterone signaling in the early nephropathy of rats with metabolic syndrome: possible contribution of fat-derived factors. J Am Soc Nephrol 17:3438–3446
27. Ohtaka A, Ootaka T, Sato H, Ito S (2002) Phenotypic change of glomerular podocytes in primary focal segmental glomerulosclerosis: developmental paradigm? Nephrol Dial Transplant 17(Suppl 9):11–15
28. Pavenstadt H, Kriz W, Kretzler M (2003) Cell biology of the glomerular podocyte. Physiol Rev 83:253–307
29. Reiser J, Kriz W, Kretzler M, Mundel P (2000) The glomerular slit diaphragm is a modified adherens junction. J Am Soc Nephrol 11:1–8
30. Rhyu DY, Yang Y, Ha H, Lee GT, Song JS, Uh ST, Lee HB (2005) Role of reactive oxygen species in TGF-beta1-induced mitogen-activated protein kinase activation and epithelial–mesenchymal transition in renal tubular epithelial cells. J Am Soc Nephrol 16:667–675
31. Robinson K, Gupta A, Dennis V, Arheart K, Chaudhary D, Green R, Vigo P, Mayer EL, Selhub J, Kutner M, Jacobsen DW (1996) Hyperhomocysteinemia confers an independent increased risk of atherosclerosis in end-stage renal disease and is closely linked to plasma folate and pyridoxine concentrations. Circulation 94:2743–2748
32. Sam R, Wanna L, Gudehithlu KP, Garber SL, Dunea G, Arruda JA, Singh AK (2006) Glomerular epithelial cells transform to myofibroblasts: early but not late removal of TGF-beta1 reverses transformation. Transl Res 148:142–148
33. Sen U, Basu P, Abe OA, Givvimani S, Tyagi N, Metreveli N, Shah KS, Passmore JC, Tyagi SC (2009) Hydrogen sulfide ameliorates hyperhomocysteinemia-associated chronic renal failure. Am J Physiol Renal Physiol 297:F410–F419
34. Sen U, Moshal KS, Tyagi N, Kartha GK, Tyagi SC (2006) Homocysteine-induced myofibroblast differentiation in mouse aortic endothelial cells. J Cell Physiol 209:767–774

35. Skoberne A, Konieczny A, Schiffer M (2009) Glomerular epithelial cells in the urine: what has to be done to make them worthwhile? Am J Physiol Renal Physiol 296:F230–F241
36. Sun X, Fang Z, Zhu Z, Yang X, He F, Zhang C (2009) Effect of down-regulation of TRPC6 on the puromycin aminonucleoside-induced apoptosis of mouse podocytes. J Huazhong Univ Sci Technolog Med Sci 29:417–422
37. Susztak K, Raff AC, Schiffer M, Bottinger EP (2006) Glucose-induced reactive oxygen species cause apoptosis of podocytes and podocyte depletion at the onset of diabetic nephropathy. Diabetes 55:225–233
38. Thiery JP (2003) Epithelial–mesenchymal transitions in development and pathologies. Curr Opin Cell Biol 15:740–746
39. Tobar N, Villar V, Santibanez JF (2010) ROS-NFkappaB mediates TGF-beta1-induced expression of urokinase-type plasminogen activator, matrix metalloproteinase-9 and cell invasion. Mol Cell Biochem 340:195–202
40. Tyagi N, Moshal KS, Sen U, Vacek TP, Kumar M, Hughes WM Jr, Kundu S, Tyagi SC (2009) H2S protects against methionine-induced oxidative stress in brain endothelial cells. Antioxid Redox Signal 11:25–33
41. Wharram BL, Goyal M, Wiggins JE, Sanden SK, Hussain S, Filipiak WE, Saunders TL, Dysko RC, Kohno K, Holzman LB, Wiggins RC (2005) Podocyte depletion causes glomerulosclerosis: diphtheria toxin-induced podocyte depletion in rats expressing human diphtheria toxin receptor transgene. J Am Soc Nephrol 16:2941–2952
42. Yi F, dos Santos EA, Xia M, Chen QZ, Li PL, Li N (2007) Podocyte injury and glomerulosclerosis in hyperhomocysteinemic rats. Am J Nephrol 27:262–268
43. Yi F, Jin S, Zhang F, Xia M, Bao JX, Hu J, Poklis JL, Li PL (2009) Formation of lipid raft redox signalling platforms in glomerular endothelial cells: an early event of homocysteine-induced glomerular injury. J Cell Mol Med 13:3303–3314
44. Yi F, Li PL (2008) Mechanisms of homocysteine-induced glomerular injury and sclerosis. Am J Nephrol 28:254–264
45. Yi F, Xia M, Li N, Zhang C, Tang L, Li PL (2009) Contribution of guanine nucleotide exchange factor Vav2 to hyperhomocysteinemic glomerulosclerosis in rats. Hypertension 53:90–96
46. Yi F, Zhang AY, Janscha JL, Li PL, Zou AP (2004) Homocysteine activates NADH/NADPH oxidase through ceramide-stimulated Rac GTPase activity in rat mesangial cells. Kidney Int 66:1977–1987
47. Yi F, Zhang AY, Li N, Muh RW, Fillet M, Renert AF, Li PL (2006) Inhibition of ceramide-redox signaling pathway blocks glomerular injury in hyperhomocysteinemic rats. Kidney Int 70:88–96
48. Yu D, Petermann A, Kunter U, Rong S, Shankland SJ, Floege J (2005) Urinary podocyte loss is a more specific marker of ongoing glomerular damage than proteinuria. J Am Soc Nephrol 16:1733–1741
49. Zhang C, Hu JJ, Xia M, Boini KM, Brimson CA, Laperle LA, Li PL (2010) Protection of podocytes from hyperhomocysteinemia-induced injury by deletion of the gp91phox gene. Free Radic Biol Med 48:1109–1117
50. Zhang C, Hu JJ, Xia M, Boini KM, Brimson C, Li PL (2010) Redox signaling via lipid raft clustering in homocysteine-induced injury of podocytes. Biochim Biophys Acta 1803:482–491
51. Zhang C, Jiang HJ, Chang Y, Fang Z, Sun XF, Liu JS, Deng AG, Zhu ZH (2009) Downregulation of CD2-associated protein impaired the physiological functions of podocytes. Cell Biol Int 33:632–639
52. Zhang DX, Zou AP, Li PL (2003) Ceramide-induced activation of NADPH oxidase and endothelial dysfunction in small coronary arteries. Am J Physiol Heart Circ Physiol 284:H605–H612
53. Zou J, Yaoita E, Watanabe Y, Yoshida Y, Nameta M, Li H, Qu Z, Yamamoto T (2006) Upregulation of nestin, vimentin, and desmin in rat podocytes in response to injury. Virchows Arch 448:485–492